Air-loads Prediction of a UH-60A Rotor inside the 40- by 80-Foot Wind Tunnel

I-Chung Chang
Aerospace Engineer
NASA Ames Research Center
Moffett Field, California
I.C.Chang@nasa.gov

Ethan A. Romander
Aerospace Engineer
NASA Ames Research Center
Moffett Field, California
Ethan.Romander@nasa.gov

Mark Potsdam
Aerospace Engineer
Aeroflightdynamics Directorate, U. S. Army
Moffett Field, California
mark.potsdam@us.army.mil

Hyeonsoo Yeo
Aerospace Engineer
Aeroflghtdynamics Directorate, U. S. Army
Moffett Field, California
hyeonsoo.yeo@us.army.mil

ABSTRACT

The presented research extends the capability of a loose coupling computational fluid dynamics (CFD) and computational structure dynamics (CSD) code to calculate the flow-field around a rotor and test stand mounted inside a wind tunnel. Comparison of predicted air-load results for a full-scale UH-60A rotor recently tested inside the National Full-Scale Aerodynamics Complex (NFAC) 40- by 80-Foot Wind Tunnel at Ames Research Center and in free-air flight are made for three challenging flight data points from the earlier conducted UH-60A Air-loads Program. Overall results show that the extension of the coupled CFD/CSD code to the wind-tunnel environment is generally successful.

INTRODUCTION

Accurate and efficient helicopter flow-field and air-loads prediction is a challenge for CFD research. The flow-field is unsteady, three-dimensional, with transonic flow in the first quadrant of the rotor azimuth, reverse flow in the third quadrant, and vortical wakes underneath of the rotor. In addition, rotor blades are subjected to complex aero-elastic interactions and elastic deflections. It thus requires a multi-disciplinary approach to satisfactorily couple computational fluid dynamics (CFD) and computational structure dynamics (CSD) tools to calculate the flow-field.

One earlier approach to couple both CFD and CSD codes was introduced by Tung, Caradonna, and Johnson [1] using a transonic small disturbance flow code (FDR) and a rotorcraft comprehensive code (CAMRAD). Other transonic small disturbance (TSD) codes [2] and full-potential flow (FP) codes [3, 4, 5] were later coupled by researchers with not only CAMRAD code but also other comprehensive rotorcraft codes. In this methodology, the CFD code requires not only blade deflections but inflow angles from the comprehensive rotorcraft analysis code to account for rotor blade structural deformation and the influence of the wake outside the very small CFD computational domain (usually limited to the outboard portion of the blade and a few chords away). Issues were encountered and overcome with the convergence of the coupled code as well as accurately estimating the rotor inflow angles.

With the continuing advancement of computational power, it has become possible to use both Euler codes [6] and Navier-Stokes CFD codes [7, 8, 9, 10] for the CFD portion of the coupled CFD/CDS toolset. The prediction of full domain rotor wakes in these codes no longer requires the added complexity of estimating inflow angles outside the computational domain, instead relying on a direct simulation of the entire flow field. One of the best examples in this category is the coupled code recently developed by Potsdam, Yeo, and Johnson [11]. The CFD code used is a NASA developed Reynolds-averaged Navier-Stokes code, OVERFLOW2 [12], which has been applied to a wide range of fluid dynamics problems including rotorcraft problems. The CSD code employed is the well-known comprehensive rotorcraft analysis code, CAMRADII [13], which has been extensively used at NASA as well as in the U.S. helicopter industry.

Recently, a full-scale wind-tunnel test of a UH-60A rotor was completed in the National Full-Scale Aerodynamics Complex (NFAC) 40- by 80-Foot wind tunnel (40-by-80) to evaluate the potential of Individual Blade Control (IBC): to improve rotor aerodynamic performance; to reduce vibration, loads and noise; and to improve flight control

Presented at the American Helicopter Society Aeromechanics Specialist' Conference, San Francisco, California, January 20-22, 2010.

characteristics [14]. A considerable body of experimental data was acquired. Validation of CFD and CSD codes using this experimental data is an important step in the advancement in prediction techniques. In addition to the NFAC test data, there is also complementary flight test data from the UH-60A Air-loads Program [15] to correlate with.

Therefore the objective of current computational work is to extend the capability of the coupled OVERFLOW2 and CAMRADII code, originally developed for studies of a helicopter rotor in free-air flight, to include the calculation of the flow-field around a rotor and test stand mounted inside a wind tunnel so as to accurately account for the influence of test stand and tunnel-wall interference effects. The large rotor test apparatus (LRTA) test stand will ultimately be included in the wind tunnel CFD modeling, However in this paper, only an isolated UH-60A rotor (without test stand) inside the 40- by 80-Foot Wind Tunnel is modeled in flow calculations.

There are three particularly challenging flight conditions in the flight test data of the UH-60A Air-loads Program which are of concern in this paper. These three flight test conditions are: 1) high speed with advancing blade negative lift (labeled with the identifier C8534), 2) low speed with blade-vortex interaction (C8513), and 3) high thrust with dynamic stall (C9017). The focus of the following work is the validation of the newly developed coupled code by comparing its rotor air-loads results predicted inside the wind tunnel with that predicted in free-air flight for the above three cases. In order to simplify the wind tunnel modeling for this paper, the test stand is excluded from the flow calculations.

OVERFLOW2 MODELING

The UH-60A rotor is a 4-bladed rotor. The rotor has a radius of 26.83 feet. The rotor description, with aerodynamic and structural properties, can be found in the UH-60A master input data [15]. A computational grid system of the UH-60A rotor virtually mounted inside the 40- by 80-Foot wind tunnel is generated by the OVERGRID code [16]. The grid system consists of 13 grids with more than 6.5 million grid points as shown in Fig. 1. The 40- by 80-Foot Wind Tunnel is modeled in a simplified sense as a straight tunnel section of length 20.28 rotor-tip radius (long side of the wind tunnel), with the cross section dimensions exactly as that of the test section. The UH-60A rotor hub center is located at the center of cross plane of 6.75 rotor-tip radii down-stream away from the wind tunnel entrance plane The wind tunnel grid has mesh-point dimensions of 226x206x99 (chord-wise, span-wise, normal).

The mesh points of the grid are not evenly distributed. They are instead clustered around the rotor blades, and at both the entrance and the exit of wind tunnel test section for better flow solutions. For each of the four UH-60A blades, three near-body grids define the blade, root cap, and tip cap. These near-body grids extend approximately about one chord length away from the surface and include sufficient resolution to capture boundary layer viscous effects. Blade and both cap grids use a C-mesh topology. The main blades have mesh-point dimensions of 125x82x33. The root caps have mesh-point dimensions of 56x31x33. The tip caps have mesh-point dimensions of 69x31x33. Each component of the rotor blade is well defined by the X-ray software, GENX [17], so that the domain connectivity, hole cuts, and inter-grid boundary point interpolation coefficients, at each time step as the near-body grids move through the stationary wind-tunnel grid, can be established.

In all CFD calculations, the grid system uses single fringing. The OVERFLOW2 results use 2^{nd} order spatial central differencing with standard 2^{nd} and 4^{th} -order artificial dissipation and implicit 2^{nd} -order temporal scheme with 5 spatial sub-iterations for each quarter degrees time step in all grids. The sub-iteration schemes allow a bigger time step for numerical stability. Viscous flow boundary conditions with the Spalart-Allmaras turbulence model are used in the rotor near-body grids. Inviscid flow boundary conditions are applied at the wind-tunnel grid. Uniform free-stream conditions are prescribed at the tunnel entrance plane. Conservation of mass condition is enforced at the tunnel exit plane [18].

LOOSE COUPLING METHODOLOGY

The fundamental concept of the loose coupling procedure introduced in the seminal paper [1] is that the methodology replaces the air-loads of a comprehensive rotorcraft analysis code with the air-loads predicted by a CFD code in an iterative way, while using a lifting line aerodynamic analysis to trim the rotor and a blade dynamic analysis to predict rotor blade deformation motion. This basic idea is further implemented in previous work [11] as follow.

0-th Coupling

The coupling calculation is initialized with the CAMRADII code using lifting line aerodynamics, resulting a trimmed rotor solution. This run estimates initial quarter-chord motion and chord-wise twist as a function of radius and azimuth, the results of which are transferred to the OVERFLOW2 code. Because OVERFLOW2 models the entire rotor domain, including all blades and full wakes, there are no other required inputs from the CAMRADII code to the OVERFLOW2 code. This eliminates the need for ad hoc inflow angles or induced velocity effects as required in

earlier work with potential flow codes or Navier-Stokes codes with partial flow-domain methodologies.

The OVERFLOW2 code is run using the CAMRADII specified blades motions. This initial CFD solution need not be fully converged, typically, one full rotor revolution (360 degrees) is sufficient. OVERFLOW2 outputs normal force (NF), pitching moment (PM), and chord-wise force (CF) as a function (one-revolution CFD solution) of radius and azimuth at user-specified intervals, typically each one degrees azimuth increment. These forces and moments are then passed back to CAMRADII for the next coupling iteration.

N-th Coupling

Thereafter, the aerodynamic forces and moments (F/M) that are used in the CAMRADII code at the next (N-th) iteration are the CAMRADII lifting line solution required to trim the rotor plus a correction based on OVERFLOW2 code. To be specific, this correction is the difference between the previous OVERFLOW2 and CAMRADII solutions.

In alternative reformation, the F/M used in the CAMRADII code are those F/M computed by OVERFLOW2 code plus an increment of F/M required to re-trim the rotor. The increment, identified as a trim correction, should generally be small, and all that is required is that the trends of the C81-table look-up be relatively consistent with the CFD. There is a possibility that the CAMRADII lifting line aerodynamic analysis will move the solution in wrong direction. For example, this might be expected when parts of the rotor are stalled.

With new iterations of quarter-chord motions of the re-trimmed rotor from CAMRADII, the OVERFLOW2 code is successively run. For a 4-bladed rotor, only one quarter of a revolution (90 degrees) is usually sufficient. Again, it is not necessary to fully converge the flow solution in the sense of iterative relaxation. New OVERFLOW2 results are then passed back to the CAMRADII code to complete the current coupling iteration.

This coupling iteration is repeated several times until that the collective and cyclic angles in the CAMRADII code, and the OVERFLOW2 predicted aerodynamic forces do not change more than the prescribed threshold values between two iterations. Upon convergence, the total air-loads used in the CAMRADII code are the OVERFLOW2 air-loads.

Trim Conditions

For the three forward flight cases noted earlier, the CAMRADII code is used to trim. In each case, CAMRADII solves for the collective and cyclic controls with respect to the specified measured rotor thrust (lb, up for positive value), hub roll moment (ft-lb, right wing down for positive value), and hub pitch moment (ft-lb, nose up for positive value) with a prescribed rotor shaft pitch angle (deg, nose up for positive value).

Using the above coupling procedure is exactly followed here in the present work. Results are generated for an isolated UH-60A rotor in both wind-tunnel environment and free-air flight for the same flight conditions,

RESULTS

Three level flight UH-60A data points (defined in Table 1) have been selected to represent the wide range of helicopter flight and wind tunnel test conditions. They are again: 1) high speed with advancing blade negative lift (C8534), 2) low speed with blade-vortex interaction (C8513), and 3) high thrust with dynamic stall (C9017). Air-loads predicted inside the wind-tunnel environment are compared with that predicted in the free-air flight for these three cases.

For 0-th coupling iteration as defined earlier, it takes one full revolution, 360 degrees, to establish the CFD flow field. After that, for N-th coupling iteration only 90 degrees in azimuth need be advanced/stepped through computationally for a 4-bladed rotor to get reasonably converged one-revolution CFD solution.

High Speed (C8534)

Flight counter C8534 is a high-speed level flight test point flown at 3271.5 feet (pressure altitude). The hover tip Mach number of the UH-60A rotor is approximately 0.642. The free-stream Mach number of this point is 0.236. This results in an advance ratio of 0.37.

The OVERFLOW2/CAMRADII code trims the rotor and solves for the collective and cyclic controls to get the measured thrust of 16602 lb, hub roll moment of -6042 ft-lb, and hub pitch moment of -4169 ft-lb with rotor shaft angle fixed at -7.31 degrees.

Comparisons of the predicted blade air-loads of the rotor inside the wind tunnel with that of the rotor in free-air flight are shown in Fig. 2. Overall differences of the predicted normal forces and pitch moments at three radial stations (r/R = 0.675, 0.865 and 0.965) are very small for this high-speed flight test condition. Advancing blade negative lift is confirmed for both wind-tunnel environment and free-air flight calculations. Two mean (averaged over all predicted azimuth angles) normal force distributions along blade span

are very close to each other as shown in Fig. 3. However, there is a minor difference in rotor tip region. Which may indicate that the rotor tip loss is larger for the wind-tunnel case. A comparison of two power prediction iterative histories shows little difference in Fig. 4.

Low Speed (C8513)

Flight counter C8513 is a low-speed level flight test point flown at 2145.9 feet. The free-stream Mach number is 0.096. The hover tip Mach number is 0.644. The advance ratio is 0.15. At this condition, significant blade-vortex interactions dominate the air-loads of the rotor blades

The OVERFLOW2/CAMRADII code trims the rotor and solves for the collective and cyclic controls to get the measured thrust of 16104 lb, hub roll moment of -958 ft-lb, and hub pitch moment of -5470 ft-lb at a fixed rotor shaft angle of 0.75 degrees.

Comparisons of the predicted air-loads of the isolated rotor inside the wind tunnel and in free-air flight are shown in Fig. 5. The predicted normal force distributions at r/R=0.675 show substantial difference between 60 to 120 degrees. Pitch moment distributions at the same radial station confirm that there may have a blade–vortex interaction in the free-air flight. At the r/R=0.865, pitch moment distribution of the wind tunnel case indicates that one blade-vortex interaction occurs near 60 degrees azimuth. However, the blade-vortex interaction appears to occur, instead, near 75 degrees for the free-air flight. A comparison of mean normal force distributions is shown in Fig. 6. There is a small difference in rotor tip region again. It again indicates that the rotor thrust tip loss is larger for the wind tunnel case. One may draw from the two observations that thrust tip loss is due to wind-tunnel interference effects. A comparison of two power prediction histories of coupling iterations shows that the power level of the rotor in the wind-tunnel case is lower than that of the free-air flight case in Fig. 7. This is due to the wind tunnel interference effects also.

High Thrust (C9017)

Flight counter C9017 is a high-thrust, level flight test point flown at 17,000 feet. The temperature is very low at 24.761 degrees in Fahrenheit. The free-stream Mach number of this point is 0.157. The hover tip Mach number has increased to 0.665. This is a very challenging test case from a predictive standpoint due to the wide variation of unsteady flow conditions, ranging from transonic to stall, with noticeable wake interactions.

The OVERFLOW2/CAMRADII code trims the rotor and solves for the collective and cyclic controls to get the measured thrust of 16452 lb, hub roll moment of -379 ft-lb, and hub pitch moment of -138 ft-lb with a fixed rotor shaft angle of -0.15 degrees (near zero angle of attack).

A comparison of the power prediction iteration histories in Fig 8 shows that the present version of the loosely coupled code converges for the wind-tunnel case but fails to converge for the free-air flight case. One possible reason for the failed convergence could be that the Spalart-Allmaras turbulence model is used, instead of the Baldwin-Barth turbulence model, in the present calculations. The Baldwin-Barth turbulence model was applied in the previous work and did yield converged solutions for this test case [11]. Other possible reason could be due to the mesh size between the level-one grids and the wind-tunnel grid [19]. Thereafter, the comparisons are made at six coupling iterations (before the divergence) for both wind tunnel and free-air predictions. Comparisons of the air-loads of the rotor inside the wind tunnel and in free-air flight are shown in Fig. 9. Overall differences of predicted normal forces and pitch moments at three radial stations (r/R = 0.675, 0.865 and 0.965) are relatively large. However, a comparison of two mean normal force distributions shows that there is relatively small difference between them in Fig. 10. For completeness, a comparison of power iterative histories up to six coupling iterations is presented in Fig. 11. The power levels show little difference for this flight data point. Further research study is required for this flight test data point because that CFD stall prediction accuracy still needs to be improved.

Though all prediction results presented in this paper are solely for isolated rotor in either wind-tunnel environment or in free-air flight. Future work will include modeling of the LRTA test stand in the wind-tunnel calculations and the helicopter fuselage in the free-air flight simulations. As an example, Fig. 12 shows surface pressure contours on the UH-60A rotor mounted on the LRTA inside the 40- by 80-Foot Wind Tunnel.

CONCLUDING REMARKS

This present work begins with a version of a loose coupling OVERFLOW2/CAMRADII code previously demonstrated for a helicopter rotor in free-air flight conditions. The objective of the current project is to extend the capability of this coupled code to predict the air-loads of a rotor mounted inside a wind tunnel. Comparisons of computed air-load results for the UH-60A rotor both inside the 40- by 80-Foot wind tunnel and in the free-air flight,are made for three challenging flight data points from the UH-60A Air-loads Program. The following specific observations are made:

1) Overall computational results show that the extension of the loosely coupled CFD/CSD code to the wind-tunnel environment is generally successful.

2) All the calculations for the UH-60A rotor are made on a relatively coarse grid system. Future work will be performed on a finer grid system.

3) Appropriate selection of turbulence models for the C9017 flight data point remains to be resolved.

4) Wind-tunnel interference effects, as referenced to blade air-loads and rotor thrust and power, are relatively minor for the three test cases examined with the possible exception of the high thrust case (C9017), though convergence issues prohibit a definite conclusion in that regards.

REFERENCES

1. Tung, C., Caradonna, F. X., and Johnson, W. R., "The Prediction of Transonic Flows on an Advancing Rotor," American Helicopter Society 40th Annual Forum, Arlington, VA, May 1984.

2. Kim, K-C., Desopper, A., and Chopra, I., "Blade Response Calculations using Three-Dimensional Aerodynamic Modeling," Journal of the American Helicopter Society, Vol. 36, No. 1, pp.68-77, January 1991.

3. Strawn, R. C., Desopper, A., Miller, M., and Jones, A., "Correction of PUMA airloads – Evaluation of CFD prediction Methods," Paper No. 14, 15th European Rotorcraft Forum, Amsterdam, Netherlands, September 1989.

4. Strawn, R. C., and Bridgeman, J. O., "An Improved Three-Dimensional Aerodynamics Model for Helicopter Airloads Prediction," AIAA Paper 91-0767, AIAA 29th Aerospace Sciences Meeting and Exhibit, Reno, NV, January 1991.

5. Beaumier, P., "A Coupling Procedure Between a Rotor Dynamics Code and a 3D Unsteady Full Potential Code," American Helicopter Society 3rd Decennial Specialists' Conference on Aeromechanics, San Francisco, CA., January 1994.

6. Servera, G., Beaumier, P., and Costes, M., " A weak Coupling Method between the Dynamics Code Host and the 3D Unsteady Euler Code WAVES," 26th European Rotorcraft Forum, The Hague, Netherlands, September 2000.

7. Sitaraman, J., Baeder, J. D., and Chopra, I., "Validation of UH-60A Rotor Blade Aerodynamic Characteristics Using CFD," American Helicopter Society 59th Annual Forum, Phoenix, AZ., May 2003.

8. Sitaraman, J.,Datta, A., Baeder, J. D., and Chopra, I., "Fundamental Understanding and Prediction of Rotor Vibratory Loads in High-Speed Forward Flight," 29th European Rotorcraft Forum, Friedrichshafen, Germany, September 2003.

9. Pahlke, K., and van der Wall, B., "Calculation of Multi-bladed Rotors in High-Speed Forward Flight with Weak Fluid-Structure Coupling," 27th European Rotorcraft Forum, Moscow, Russia, September 2001.

10. Datta, A., Sitaraman, J., Chopra, I., and Baeder, J. D., "Improved Comprehensive Analysis for Prediction of Rotor Vibratory Loads in High-Speed Forward Flight," American Helicopter Society 60th Annual Froum, Baltimore, MD, June 2004.

11. Potsdam, M., Yeo, H., and Johnson, W., "Rotor Airloads Prediction using Loose Aerodynamics/Structural Coupling," American Helicopter Society, 60th Annual Forum, Baltimore, MD, June, 2004.

12. Nichols, R. H., and Buning, P. G., "User's Manual for OVERFLOW 2.1," August 2008

13. Johnson, W., "Rotorcraft Aerodynamic Models for a Comprehensive Analysis," American Helicopter Society 54th Annual Forum, Washington, D. C., May 1998

14. Norman, T. R., Theodore, C., Shinoda, P., Fuerst, D., Arnold, U. T. P., Makinen, S., Lorber, P., and O'Neill, J. "Full-Scale Wind Tunnel Test of a UH-60 Individual Blade Control System for Performance Improvement and Vibration, Loads and Noise Control," American Helicopter Society 65th Annual Forum, Grapevine, TX, May 2009

15. Kufeld, R. M., Balough, D. L., Cross, J. L., Studebaker, K. F., Jennison, C. D., and Bousman, W. G., "Flight Testing of the UH-60A Airloads Aircraft," American Helicopter Society 50th Annual Forum, Washington, D. C., May 1994.

16. Chan, W., Meakin, R. L., and Potsdam, M. A.,"CHSSI Software for Geometrically Complex

Unsteady Aerodynamic Applications," AIAA Paper 2001-0593, AIAA 39th Aerospace Sciences meeting and Exhibit, Reno, NV, January 2001.

17. Meakin, R. L., "Object X-Rays for Cutting Holes in Composite Overset Structure Grids," AIAA Paper 2001-2537, 15th AIAA Computational Fluid Dynamics Conference, Anaheim, CA, June 2001.

18. Rogers, S. E., and Roth K., "Validation of Computed High-Lift Flows with Significant Wind-Tunnel Effects," AIAA Journal Vol. 39, No. 10, October 2001.

19. Potsdam, M., and Pulliam, T., "Turbulence Modeling Treatment for Rotorcraft Wakes", AHS Specialists' Conference on Aeromechanics, San Francisco, CA, January 2008.

Flight counter	Rotor Speed (RPM)	Airspeed (ft/sec)	Hub Pitch (deg)	Rotor Thrust (lb)	Hub Roll Moment (ft-lb)	Hub Pitch Moment (ft-lb)
C8534	258.1	266.5	-7.31	16602	-6042	-4169
C8513	257.4	110.4	0.75	16104	-958	-5470
C9017	255.8	170.2	-0.15	16452	-379	-138

Table 1: UH-60A flight test counters

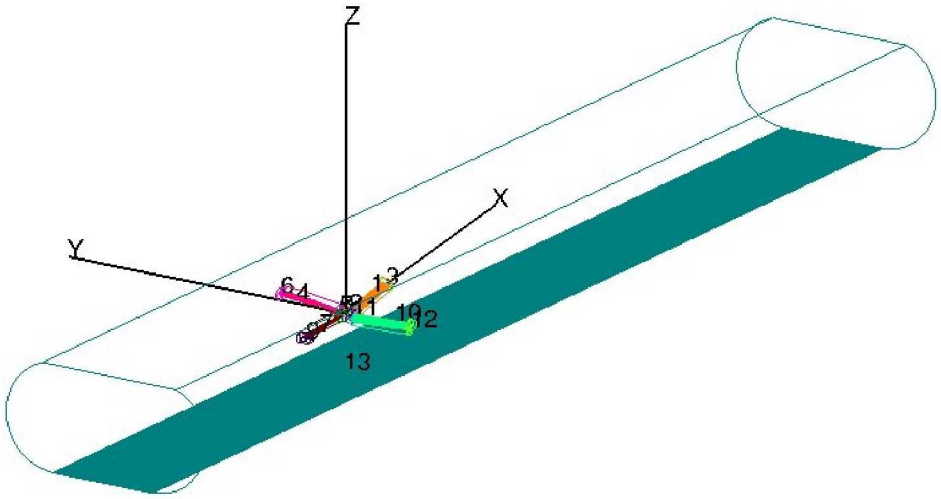

Figure 1: An overset grid system suitable for the computation of the flow field about the UH-60A rotor inside the 40-by-80 Foot Wind Tunnel consists of 13 grids with 6.5 million points.

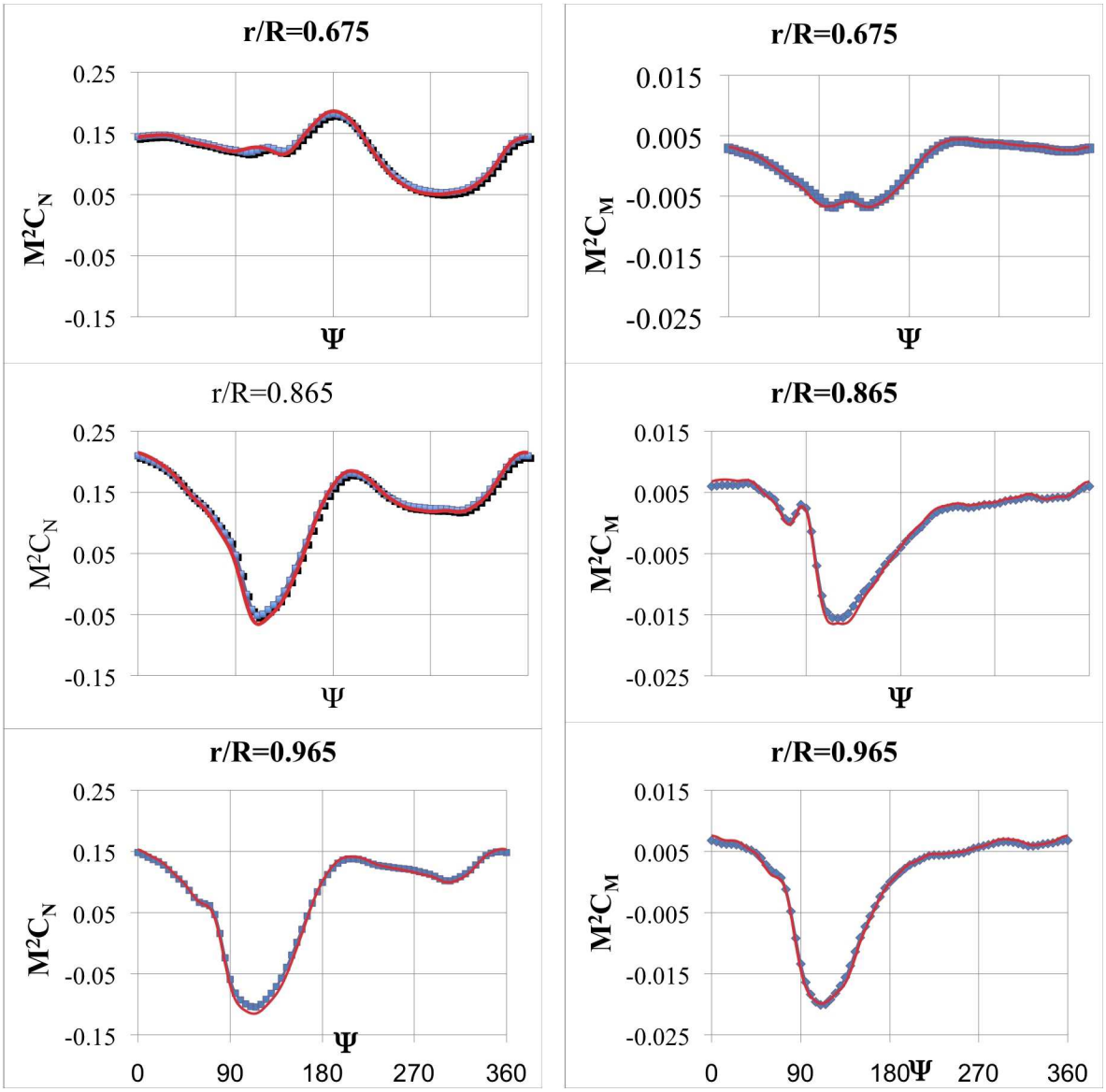

Figure 2: Air-loads comparison, C8534

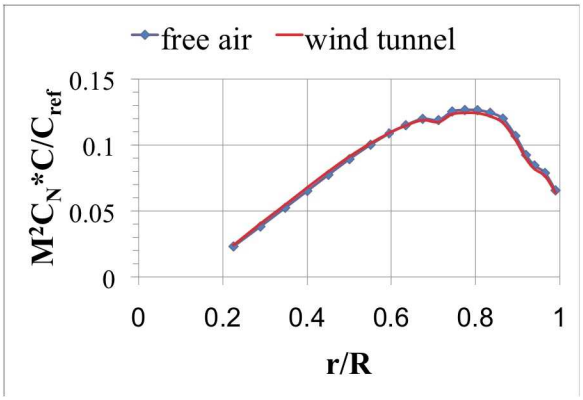

Figure 3: Mean normal force distribution, C8534

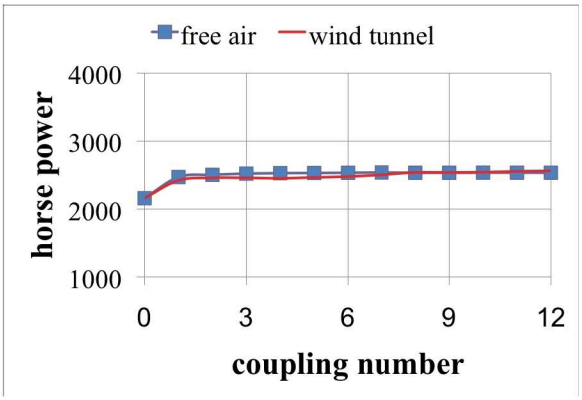

Figure 4: Power iterative history, C8534

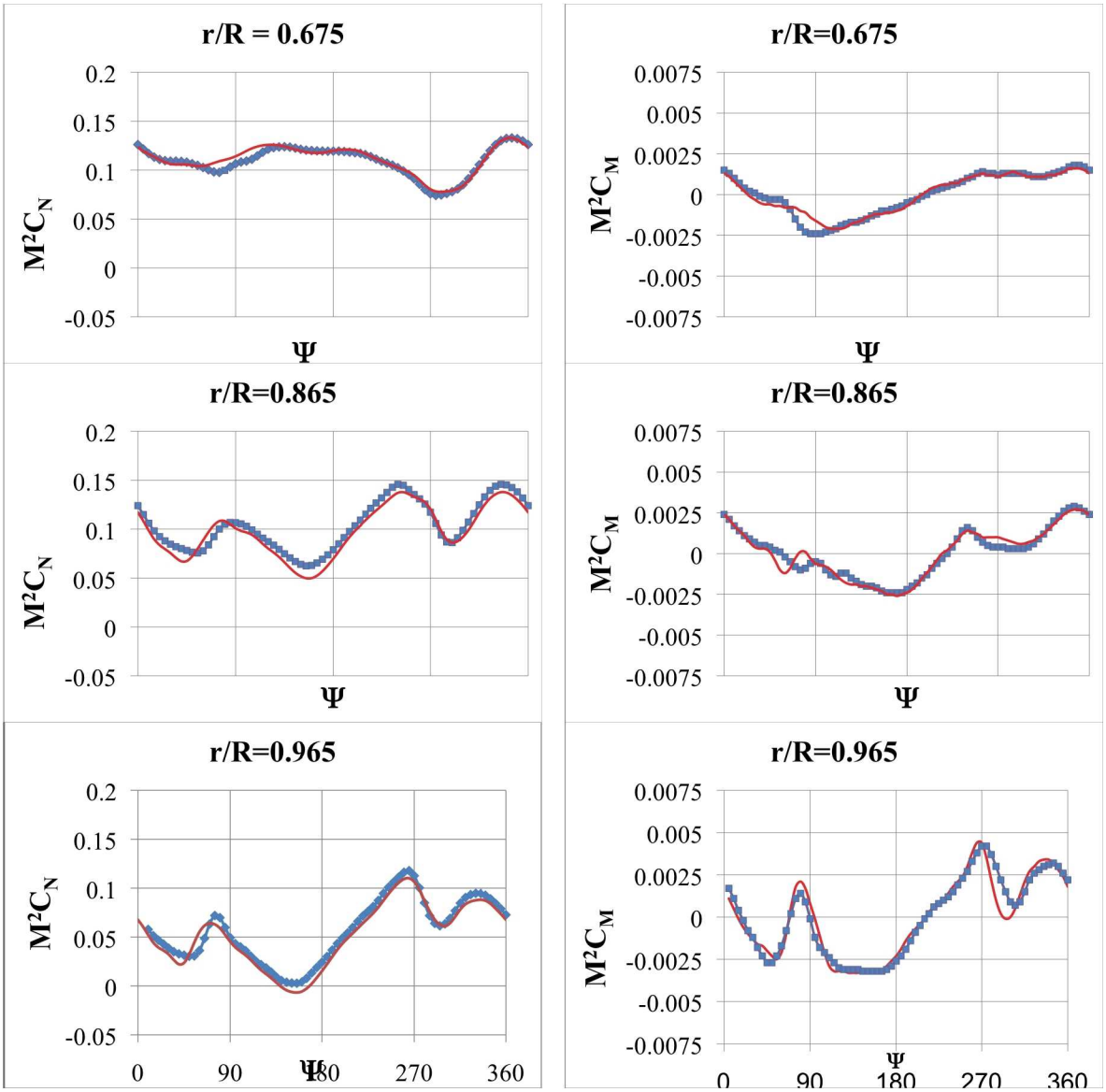

Figure 5: Air-loads comparison, C8513

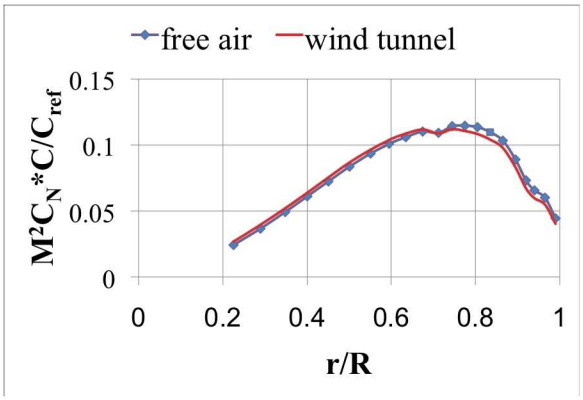

Figure 6: Mean normal force distribution, C8513

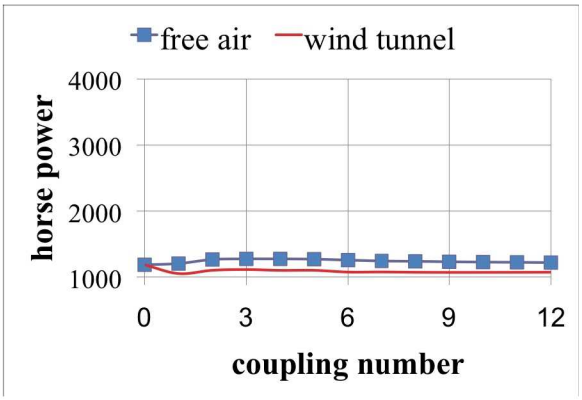

Figure 7: Power iterative history, C8513

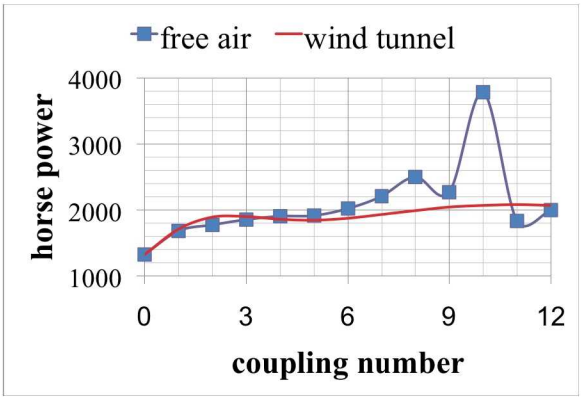

Figure 8: Power iterative history, C9017

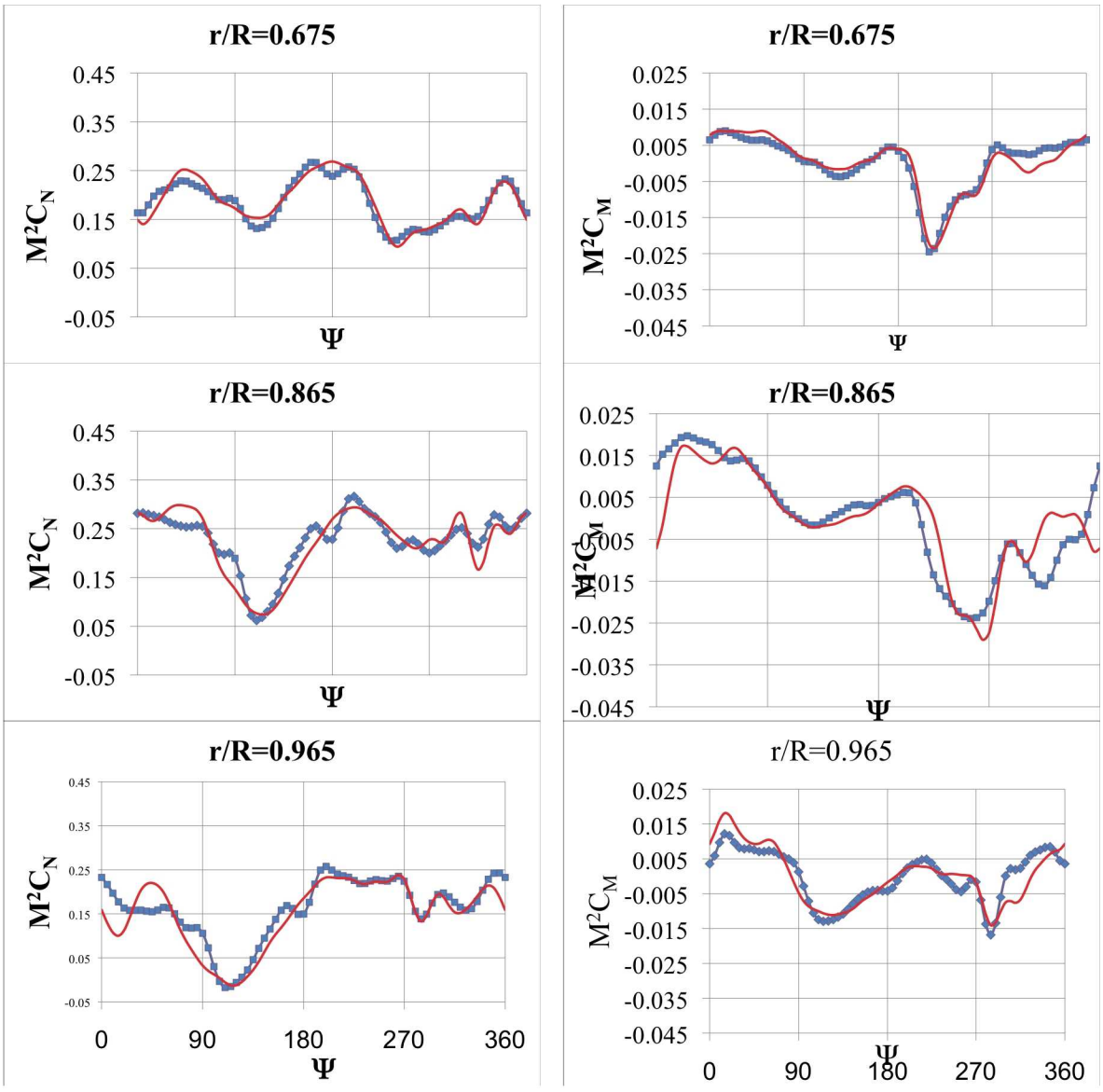

Figure 9: Air-loads comparison, C9017

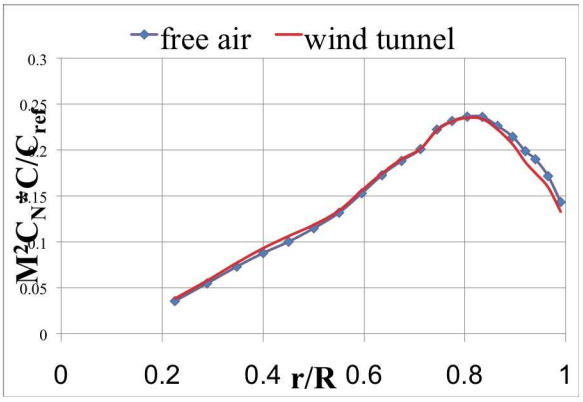

Figure 10: Mean normal force distribution, C9017

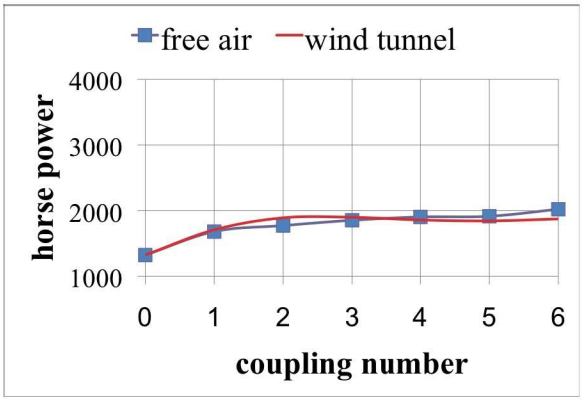

Figure 11: Power iterative history, C9017

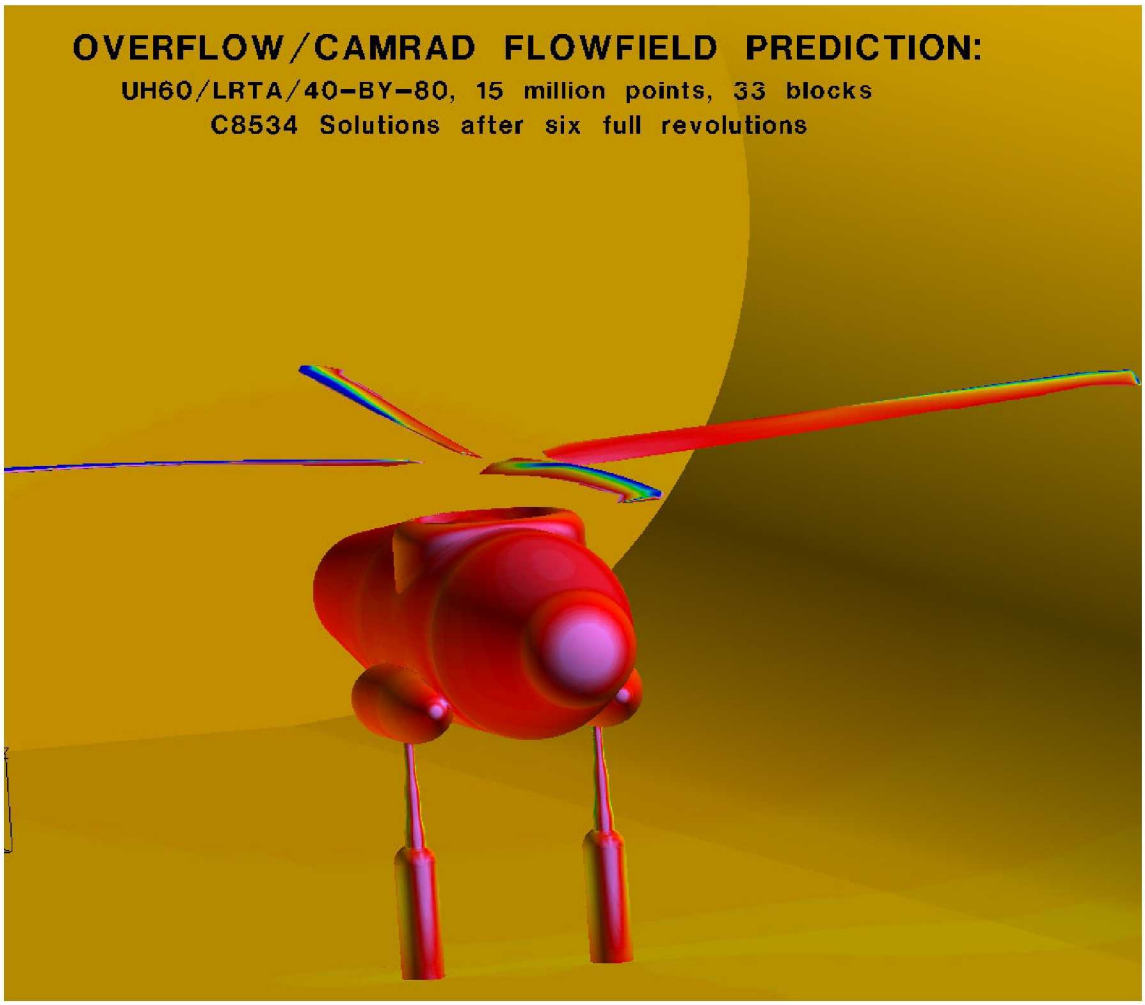

Figure 12: A snap shot of computational results for the UH-60A rotor mounted on the LRTA test stand inside the NFAC 40- by 80-Foot Wind Tunnel.